Food Biophysics (2021) 16:153–160
https://doi.org/10.1007/s11483-020-09656-6

ORIGINAL ARTICLE

3D Confocal Laser Scanning Microscopy for Quantification of the Phase Behaviour in Agarose-MCC co-gels in Comparison to the Rheological Blending-law Analysis

Pranita Mhaske[1] · Asgar Farahnaky[1] · Stefan Kasapis[1]

Received: 3 September 2020 / Accepted: 5 October 2020 / Published online: 25 October 2020

Abstract

The need for a rapid and direct alternative to the rheology-based blending laws in quantifying phase behaviour in biopolymer composite gels is explored in this study. In doing so, the efficacy of confocal laser scanning microscopy (CLSM) paired with image analysis software – FIJI and Imaris - in quantifying phase volume was studied. That was carried out in a model system of agarose with varying concentrations of microcrystalline cellulose (MCC) in comparison to the rheological blending laws. Structural studies performed using SEM, FTIR, differential scanning calorimetry and dynamic oscillation in-shear unveiled a continuous, weak agarose network supporting the hard, rod-shaped MCC inclusions where the composite gel strength increased with higher 'filler' concentration. The phase volumes of MCC, estimated with the microscopic protocol, matched the predictions obtained from computerized modelling using the Lewis-Nielsen blending laws. Results highlight the suitability of the microscopic protocol in estimating the water partition and effective phase volumes in the agarose-MCC composite gel.

Keywords Phase behaviour · Blending law analysis · 3D imaging · Confocal laser scanning microscopy · Image analysis

Introduction

The recent years have seen a drastic increase in the use of proteins and polysaccharides in food product formulations to improve/control processability, shelf life, texture/mouthfeel and the kinetics of bioactive compound release [1]. For the most part, such techno-functionality is governed by the solvent partitioning amongst the macromolecules in the phase-separated mixture [2]. Fundamental understanding of solvent distribution and molecular interactions between constituents depends on their concentration, water addition, ionic strength, pH and processing, for example, thermal treatment or applied shear. Despite the range and depth of research in the literature, a thorough understanding of phase behaviour and interactions in complex biomaterial systems remains of great interest. These systems generally comprise highly viscous and gelled phases, whose phase behaviour cannot be accurately predicted using the classical methods of centrifugal separation or determination of osmotic pressure from composite solutions [3, 4].

Other attempts to probe phase behaviour of composite systems employed turbidimetric [5], spectrometric [6] and rheological protocols. The latter, in particular, paired with blending law analysis estimated accurately the phase behaviour of synthetic and natural polymer mixtures [7, 8]. In the latter, blending laws correlate the overall mechanical properties of the composite to those of the individual constituents taking into consideration the solvent partition between the two polymeric phases. Though accurate in estimating phase volumes, their application demands considerable experimentation and modelling expertise. Clearly, there is a need for a rapid and direct approach capable of predicting the phase behaviour in biopolymer mixtures.

Over the years, confocal laser scanning microscopy (CLSM) has been used sporadically in this area and proved popular for qualitative analysis [9–11]. A few studies coupled CLSM imaging with image analysis but they were limited to the investigation of single 2D images [12] and viscous aqueous solutions [13]. Exploiting advances in image processing technology, Mhaske et al. (2019) developed a technique of quantifying phase volume in a lipid-biopolymer system using 3D CLSM imaging paired with image analysis [14]. The

✉ Stefan Kasapis
stefan.kasapis@rmit.edu.au

[1] School of Science, RMIT University, Bundoora West Campus, Plenty Road, Melbourne, VIC 3083, Australia

protocol yielded values for the volume of the lipid phase that depend entirely on its concentration (w/w) added to the system. These were in close agreement with the estimates obtained from the rheology based theoretical modelling, highlighting the potential of the combined approach.

The present work aims to quantify the phase behaviour of a complex, industrially relevant hydrogel comprising a structuring polysaccharide (agarose) and a rigid dispersion in the form of microcrystalline cellulose (MCC). The latter is also capable of absorbing and retaining water, hence being used in the cosmetics, plastic, pharmaceutical and cement industries. Applications in processed food are based on its functionality as a dietary fibre and bulking agent to manipulate the nutritional profile and consistency of preparations [15]. Thus, MCC's interactions with other biopolymers is a topic of current fundamental and applied interest. In the present system, the retention of water by agarose and MCC is unknown and yet it will go a long way in determining the structural properties of this mixture. Phase volume estimations will be attempted with the combined protocol of microscopic examination and blending law modelling in order to confirm the suitability of this approach in identifying the solvent partition between two hydrophilic polymeric phases.

Materials and Methods

Materials and Sample Preparation

Agarose (Type-1) and microcrystalline cellulose (Avicel, PH-101) were supplied by Sigma-Aldrich (Sydney, Australia). The sulphate, ash and moisture content of agarose was less than 0.15, 0.25 and 10%, respectively, according to the supplier. The particle size of cellulose crystals was ~ 50 μm, with a relative density of 0.6 g/cm^3. 5-DTAF [5-(4, 6–Dichlorotriazinyl)aminofluorescein], a bright yellow coloured powder was purchased from AAT Bioquest (California, USA) and used to covalently label agarose. Varying quantities of MCC (0.1, 0.3, 0.6, 0.9, 1.2, 1.5 g) were added to specific amounts of milliQ water to make the total volume of the aqueous solutions 99 ml. This was stood overnight at ambient temperature to ensure complete hydration of the cellulose crystals. MCC suspensions were then heated to 80 °C in a water bath with constant magnetic stirring before dispersing 1 g agarose powder. Mixtures (1% (w/w) agarose and 0.1, 0.3, 0.6, 0.9, 1.2 and 1.5% (w/w) MCC) were stirred continuously for 15 min to dissolve the polysaccharide and cooled to 50 °C for subsequent analysis.

Experimental

SEM Analysis Gel cubes of agarose (10 mm^3) with varying concentrations of MCC were freeze dried at -40 °C for 3 days in a Labconco FriZOne Triade freeze drier (Kansas City, Missouri, USA). These were then placed on 12.6 mm carbon coated aluminium stubs and gold coated. FEI Quanta 200 ESEM (Hillsboro, Oregon, USA) was used to capture the surface micrographs of the freeze dried samples. Images were captured in the high vacuum mode, with a spot size of 5, working distance of 12 mm and an accelerating voltage of 30 kV. A 50x magnification was used to obtain an overview of the gel network, whilst details of the composite topology were captured at 600 x.

Fourier Transform Infrared Spectroscopy (FTIR) A Spectrum 2 FTIR spectrometer by Perkin Elmer (Norwalk, Connecticut, USA) with a diamond crystal attenuated total reflectance device from GladiATR (Pike Technologies, Maddison, Wisconsin, USA) was used to analyse single and binary mixtures of agarose and MCC. The absorbance spectra were obtained at a resolution of 4 cm^{-1} between 400 and 4000 cm^{-1} and averaged over 64 scans in triplicate measurements by subtracting the spectrum of water.

Differential Scanning Calorimetry (DSC) Thermal analysis of agarose and agarose-MCC mixtures was carried out using the Setaram Micro DSC VII (Setu-rau, Caluire, France). About 700 mg sample was transferred into a cylindrical vessel and sealed, with an equal weight of milliQ water being added to the reference vessel. Both vessels were then deposited into the instrument chamber and held at 40 °C for 30 min before ramping the temperature to 70 °C, cooling to 5 °C and once again heating to 70 °C. Averaged exotherms from triplicate runs, obtained at a constant scan rate of 1 °C/min, are reported. MCC paste, obtained by hydrating MCC overnight in excess water and centrifuging the suspension, was also analysed using a modulated DSC Q2000 (TA Instruments, New Castle, DE, USA). The instrument was interfaced to a refrigeration unit to achieve temperatures well below 0 °C and a nitrogen purge at a flow rate of 25 mL/min was used. About 12 mg of sample was weighed in an aluminium pan and hermetically sealed, with an empty pan being the reference. Samples were subjected to successive heating and cooling routines between 10 and 350 °C at a constant scan rate of 1 °C/min. Triplicate runs produced consistent results.

Rheological Measurements Small-deformation dynamic oscillation in-shear was carried out on a Discovery Hybrid Rheometer (TA Instruments, New Castle, DE, USA) to measure the elastic modulus (G′) of the hydrated MCC paste, agarose gel and agarose-MCC composites. Samples were loaded at 50 °C onto the preheated Peltier plate with a 40 mm parallel plate geometry and 1 mm gap. The exposed edges of the composite were coated with polydimethylsiloxane (PDMS) to

minimise moisture loss. Analysis involved a temperature sweep from 50 to 5 °C at 2 °C/min, a 30 min isothermal step at 5 °C with a frequency of 1 rad/s, followed by a frequency sweep from 0.1 to 100 rad/s prior to ramping the temperature to 70 °C with a controlled strain of 0.01% throughout, which is within the linear viscoelastic region of this matrix (LVR).

Confocal Laser Scanning Microscopy (CLSM) and Image Analysis Agarose was covalently labelled with 5-DTAF (5-(4, 6-Dichlorotriazinyl) Aminofluorescein) using the procedure outlined by Russ et al. (2013) [16]. In doing so, 1 g of agarose was dissolved in 50 ml milliQ water at 80 °C with constant stirring. The solution was cooled to 60 °C and 8 mg 5-DTAF was added before slowly adding 15 ml of 1% (w/v) Na_2SO_4. Then, 3–4 drops of 10% (w/v) NaOH were added and stirred for 2 hours prior to adding 120 ml absolute ethanol to obtain a yellow precipitate. The mixture was refrigerated at -20 °C for 15 min before filtering it and washing the residue with absolute ethanol. The residue was then dried to obtain a fine yellow agarose powder.

The 5-DTAF-labelled agarose was used to make samples as outlined earlier. These were transferred into the well of a CoverWell imaging chamber (diameter – 20 mm; depth – 2.8 mm) and precooled to 4 °C to ensure rapid gelation of agarose before the settling of cellulose crystals. Nikon A1R laser fitted to an inverted microscope, ECLIPSE Ti-E (Minato, Tokyo, Japan) was used to obtain confocal images. An argon laser at 488 nm was used to excite the 5-DTAF-labelled agarose and the emissions were recorded between 500 and 530 nm. Fifteen 8-bit images, 1279 µm x 1279 µm in size were captured along the Z-axis, at an interval of 5.72 µm. The distribution of MCC from 9 different regions across the samples was studied.

Two image analysis software, Imaris 9.1.0 (Bitplane, Belfast, Northern Ireland) and FIJI with Java 6 (Madison, Wisconsin, USA) were used to quantify the Z-stacks obtained in parallel. The MCC phase volume was determined using the steps outlined by Mhaske et al. (2019) [14]. In Imaris, the Z-stack was opened in the "Surfaces" feature. A Gaussian filter was applied before subtracting the background intensity to smoothen the image and reduce noise. The volume of hollow spaces within the agarose network, attributed to the presence of unstained MCC particles, was measured. In FIJI, the "Default" algorithm was used to threshold the images, and the images were inverted to make the unstained MCC particles the object and the agarose phase the background. The area of the object pixels was calculated for the Z-stack and then multiplied by the Z-step to get the volume of the MCC particles. Results obtained for the nine images captured across each sample were averaged before reporting the phase volume of the MCC particles.

Statistical Analysis Phase volume results obtained were evaluated using Minitab 18 (Minitab Inc., Pennsylvania, USA) by one-way analysis of variance (ANOVA). Volume measurement is done in duplicate and expressed in mean ± standard deviation, with significant differences being $p < 0.05$ (Tukey test).

Results and Discussion

Structural Characterisation of the Agarose/MCC Mixtures

Scanning electron microscopy is a technique capable of providing tangible evidence on the morphology of biomaterials [17], and it is used in the present work to visualise the structure of agarose/MCC composites. As shown in Fig. 1a, agarose exhibits a highly porous, honeycomb like assembly under a low magnification of 50x. This assembly remains unchanged upon addition of MCC (images not shown), indicating that the gelation of the polysaccharide is independent of the presence of the cellulose crystal. The presence of MCC particles could not be seen at 50x magnification, which prompted us to increase it to 600x. As depicted in Fig. 1b, the walls of the agarose network appear uninterrupted and smooth at the higher magnification. Addition of MCC results in the development of rough surfaces, with rod-like MCC particles being embedded within the featureless background (Fig. 1c, d). As the concentration of MCC is raised from 0.6 to 1.2% (w/w), the surface roughness corresponding to the volume of MCC particles entrapped in the polysaccharide mesh also increases. SEM micrographs suggest that the topology of the composite gel consists of agarose strands forming a continuous matrix that supports the dispersed rod-shaped particles of the MCC filler.

Infrared spectroscopy was employed next to record the chemical fingerprints of agarose, MCC and their composites (Fig. 2). The former featured characteristic absorbance bands at 3650 cm^{-1} (O-H stretching), 2980 and 2900 cm^{-1} (C-H vibration), 1396 cm^{-1} (C-C bending), 1246 cm^{-1} (sulphate esters), 1068 cm^{-1} (C-O-C vibration of 3,6-anhydro-galactose bridges) and 877 cm^{-1} (anomeric carbon's angular C-H deformation) [18, 19]. MCC interferograms showed the general attributes of cellulose, reproducing typical absorbance bands at 1059 cm^{-1} (ring vibration and C-OH bending), 1160 cm^{-1} (C-O and C-O-C stretching), 1640 cm^{-1} (-O- tensile vibration neighbouring H atoms) and a broad band between 3225 and 3350 cm^{-1} (stretching vibrations of O-H groups) [20–22]. Composites reproduced the absorbance bands of both individual components, with no variation in their wavenumber, hence suggesting that there is no chemical interaction between the constituents of this mixture. Furthermore, as the concentration of MCC increased in the

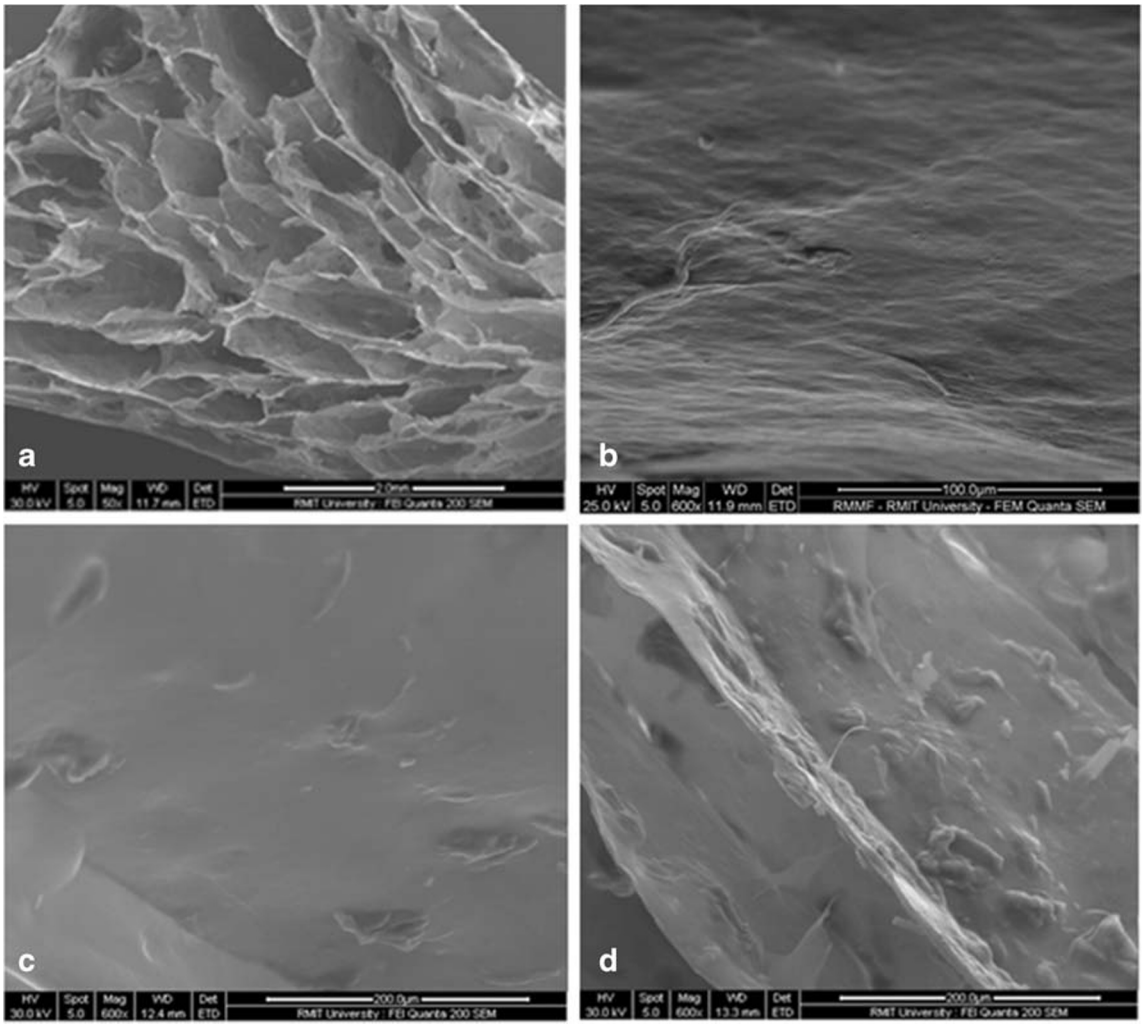

Fig. 1 SEM images of (**a**) 1% (w/w) agarose network at 50x and, walls of 1% (w/w) agarose network containing (**b**) 0, (**c**) 0.6 and (**d**) 1.2% (w/w) MCC under 600x

composite, the absorbance bands of both agarose and MCC displayed a slight amplification in intensity. This is an expected outcome, congruent with the increase in polymer concentrations in their respective domains as explained in the following sections.

In addition to infrared spectroscopy, differential scanning calorimetric tests were carried out to obtain information on the micromolecular aspects of the structural behaviour of our mixture. Featureless thermograms are recorded from the cooling cycles of the MCC paste in Fig. 3a indicating the absence of a first-order thermodynamic transition. The major features in the heating run are two endothermic peaks. The first event with a peak at about 108 °C indicates the desorption of water from the cellulose molecule, whereas the second event at 320 °C traverses the thermal decomposition of the MCC crystal [22]. Figure 3b depicts the exothermic peak of agarose upon cooling with a midpoint at 23 °C, reflecting the coil-to-helix transition of the polysaccharide leading to subsequent gel formation. Corresponding profiles of the blends also exhibit a single exothermic event that reproduces the characteristics of the agarose thermogram in terms of shape and temperature band. Once more, it is confirmed that the presence of MCC does not affect the structural properties of the agarose gel.

Finally, we studied the mechanical behaviour of single and binary mixtures of agarose and MCC. Figure 4 reproduces typical patterns of elastic modulus variation as a function of temperature when the polymer is cooled from 40 to 5 °C at a rate of 2 °C/min. A significant increase in G′ values is observed at around 35 °C (onset of gelation), approaching asymptotically an equilibrium at the end of the cooling cycle (G' is about $10^{3.8}$ Pa at 5 °C). In contrast, the storage modulus of the MCC paste produced a relatively flat pattern that remained unaffected by temperature, yielding a storage modulus value of about $10^{5.4}$ Pa (results not shown). Qualitatively, the mechanical spectra of the composite exhibit a similar trend of storage modulus development upon cooling from vestigial gelation to eventual levelling off. As the MCC concentration

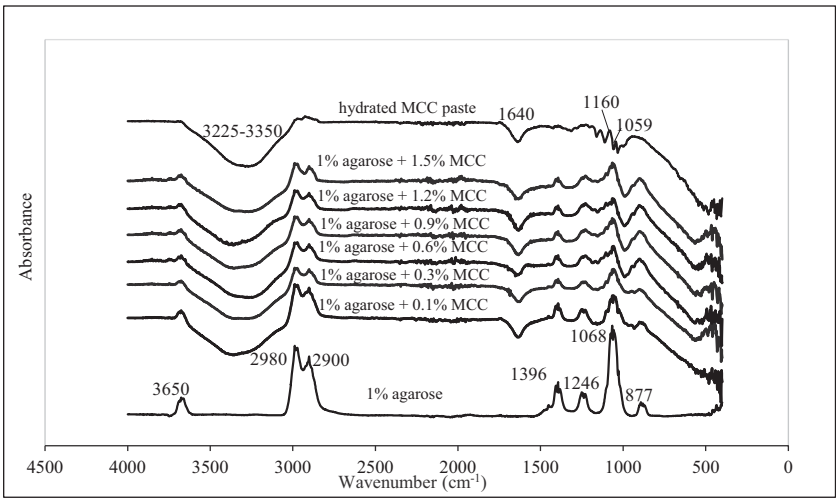

Fig. 2 FTIR spectra between 400–4000 cm^{-1} for agarose with 0, 0.1, 0.3, 0.6, 0.9, 1.2 and 1.5% (w/w) MCC and MCC by itself stacked upwards from the bottom

increases, however, so does the mechanical strength of the composite, reaching $10^{4.1}$ Pa with 1.5% (w/w) MCC addition. This outcome is partially attributed to the reinforcing effect of the hard MCC particles on the softer agarose matrix. It should also be noted that the cellulose particles absorb water [23], thereby decreasing the amount of solvent available to the agarose phase and increasing its effective concentration, an outcome that leads to the formation of a stronger hydrogel.

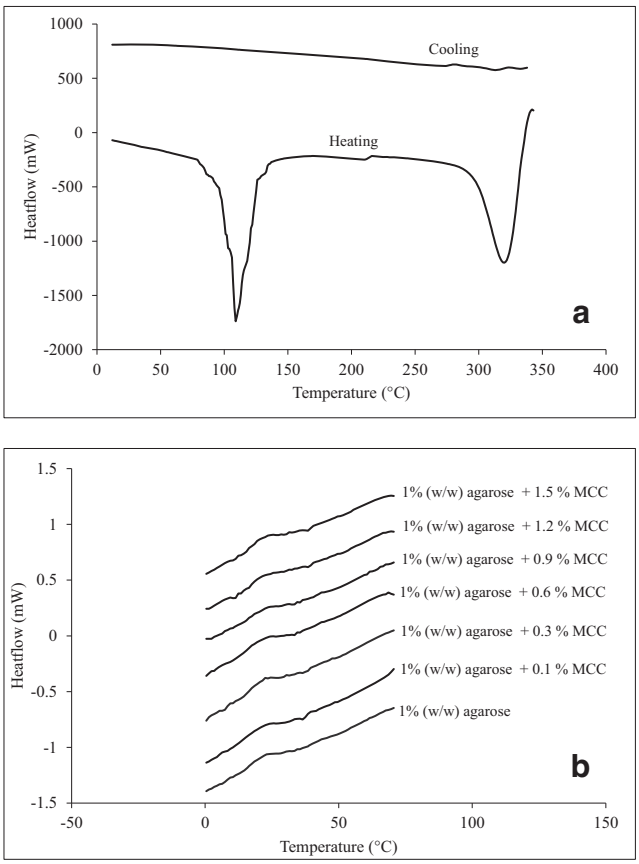

Fig. 3 DSC thermograms of (**a**) cooling and heating profiles of hydrated MCC paste and (**b**) agarose cooling profiles with 0, 0.1, 0.3, 0.6, 0.9, 1.2 and 1.5% (w/w) MCC arranged successively upwards scanned at a rate of 1 °C/min

Rheological Modelling of the Phase Behaviour in Agarose/MCC Composite Gels

Analysis thus far, established qualitatively the noninteractive nature of MCC crystal and agarose molecules leading to a filler composite with a relatively weak matrix supporting hard inclusions. We are now interested to relate quantitatively the mechanical strength of the constituent phases to the overall behaviour of the composite gel. That was initiated by obtaining a double-logarithmic calibration curve of storage modulus for the agarose network at concentrations between 1.0 to 2.5% (w/w); reported in the inset of Fig. 4. Mechanical properties were then followed by a set of equations adapted from the 'sophisticated synthetic polymer research' proposed by Lewis and Nielsen [24]:

$$\frac{G'}{G'_x} = \frac{1 + AB\Phi_y}{1 - B\psi\Phi_y} \tag{1}$$

$$B = \frac{\frac{G'_y}{G'_x} - 1}{\frac{G'_y}{G'_x} + A} \tag{2}$$

$$\psi = 1 + \left(\frac{1-\Phi_m}{\Phi_m^2}\right)\Phi_y \tag{3}$$

where, G′, G'_x, G'_y are the elastic modulus of the composite, the continuous agarose network and the discontinuous MCC phase, respectively, and ϕ_y is the phase volume of the filler. The framework considers the concept of maximum packing fraction (ϕ_m) of the filler particles, which corresponds to 0.52 for random MCC rods. The shape of the filler is taken into account *via* the Einstein co-efficient, rendering A to be 2.08 for dispersed cylindrical, rod-shaped inclusions [25].

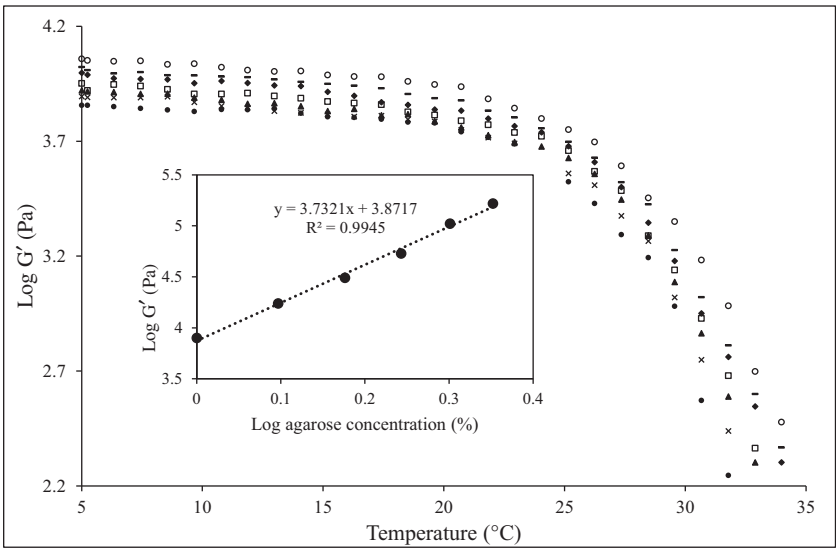

Fig. 4 Profiles of G′ for 1% (w/w) agarose with 0 (●), 0.1% (x), 0.3% (▲), 0.6% (□), 0.9% (♦), 1.2% (-) and 1.5% (○) (w/w) MCC during cooling from 50 to 5 °C at a scan rate of 2 °C/min; the agarose calibration curve of G′ at 5 °C as a function of its concentration is illustrated in the inset

In an effort to determine the contribution of each component to the elastic modulus of the composite, preparations were centrifuged at 40 °C and 10,000 rpm for 15 min. Supernatants of clear agarose solutions were decanted and their weights were recorded in order to determine the effective agarose concentration, which ranged from 1.01 to 1.08% (w/w). Respective values of G'_x for these agarose concentrations were calculated using the calibration curve from the inset of Fig. 4. Centrifuged MCC pellets were also weighed to work out the amount of absorbed water, which was ~ 4.1 times the weight of the cellulose powder in each composite. Weights of the decanted agarose supernatant and MCC pellet obtained after centrifugation were used to calculate the values of ϕ_x and ϕ_y (phase volumes of agarose and MCC, respectively) for each composite, with $\phi_x + \phi_y = 1$.

The storage modulus value of the MCC paste (about 251 kPa), obtained from rheological measurements in the preceding section, was used as a constant G'_y for all composites, with the assumption that equally hydrated MCC particles in the various composites (0.1 to 1.5% w/w MCC) would yield the same elastic response. Blending law modelling was able to produce a G' trace that exhibited a close fit with the corresponding experimental values of the composites depicted in Fig. 5, an outcome that showcases its ability to predict phase behaviour in binary composites. Corresponding volumes of the MCC phase in all composites, as predicted by blending law, are also depicted in Fig. 5 being congruent with the amount of experimentally added polysaccharide. Phase volume predictions of MCC will be compared with those obtained from microscopy, paired with image analysis, in the following section in order to assess the suitability of the microscopic protocol in quantifying phase behaviour in binary co-gels.

3D CLSM Imaging and Image Analysis for Phase Volume Estimations in the Agarose/MCC Mixture

In order to capture and then process 3D images of our composites, agarose was covalently labelled with DTAF and the procedure outlined by Mhaske et al. (2019) [14] was followed. Figure 6a depicts a typical 2D image of the surface of the gel containing 1% (w/w) agarose and 0.6% (w/w) MCC. Stained agarose forms a continuous blue background in which the unstained MCC particles are dispersed as black inclusions. This is an 8 bit 2D image with a dimension of 512 × 512 pixels, corresponding to an area of 1279 × 1279 μm. Fifteen such images were obtained along the Z-axis at a fixed interval or Z-step of 5.72 μm, reproduced in Fig. 6b, which allowed imaging the sample up to a depth of ~ 85 μm. The Z-stack was then utilized to generate a 3D image, as seen in Fig. 6c. FIJI, which is an open source analysis software, analyses the Z-stack for phase volume estimation by quantifying each 2D

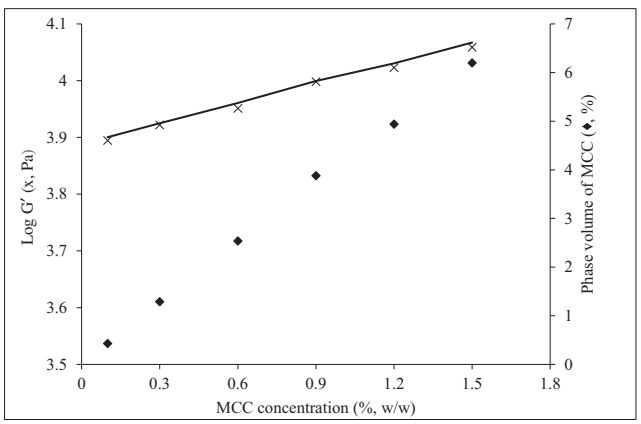

Fig. 5 Values of composite G′ obtained *via* rheological experiments (x) and blending law predictions for G' (solid line) and phase volumes of MCC (♦) for samples containing 1% (w/w) agarose with increasing MCC concentrations

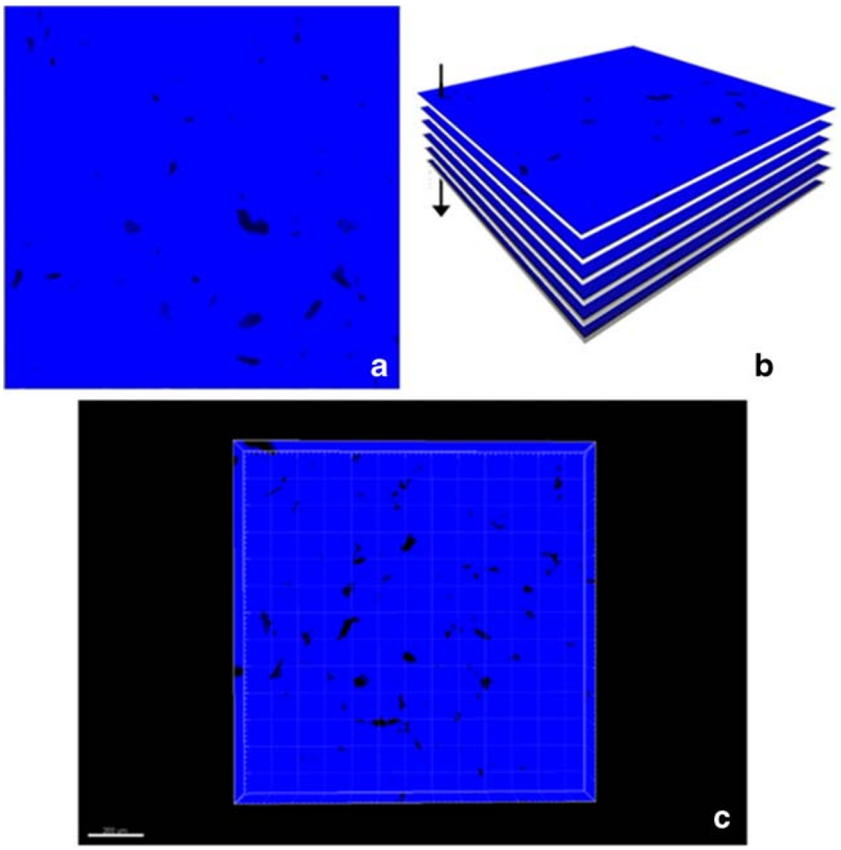

Fig. 6 (**a**) 2D, (**b**) Z-stack, and (**c**) 3D CLSM images of 1% (w/w) agarose containing 0.6% (w/w) MCC. The blue background denotes the stained agarose phase whereas the black cavities correspond to the unstained MCC particles

image separately. In contrast, Imaris renders a 3D image using the stack of 2D images before quantifying the 3D image volumetrically.

In an 8 bit image, pixels denote a specific intensity value of the wavelength emitted by the sample within the range of 0 and 255, where a pixel with the intensity of 0 appears black and refers to an unstained sample. This serves as the negative control and is considered to be the baseline calibration in image analysis [26]. Thresholding is the most critical step in image analysis in order to accurately segregate the object pixels (MCC particles) from the background pixels (agarose network) [27]. The phase volume of MCC particles in the composite was measured using the image analysis software, FIJI. Figure 7 illustrates the final phase volume of MCC in the composite in relation to the original amount of added cellulose powder. The phase volumes estimated by FIJI are comparable with those obtained from the rheological blending-law analysis in Fig. 5. Increase in the MCC phase volume in the composite also corresponds to ~4.1 times the initial added amounts documented in Fig. 7 microscopically and in Fig. 5 rheologically from the MCC concentration (%, w/w) vs.. phase volume of MCC (%) relationship. Phase volume estimations, of course, allow quantification of the amount of solvent held in a given polymeric phase.

Next, we turned our attention to the second image analysis software, Imaris. Once more the protocol used by Mhaske et al. (2019) [14] was followed to estimate the MCC phase volumes and results are also shown in Fig. 7. Similarly, the Imaris predictions are a close fit to those estimated using FIJI image analysis and rheological blending laws. Statistically, the difference between the phase volume values obtained from the two types of imaging software is not significant ($p > 0.05$) indicating that both can equally measure water absorption and its retention in the polymeric phases of the binary mixture. Nevertheless, the two types of software have distinct approaches of image quantification and their "plug-ins" vary in

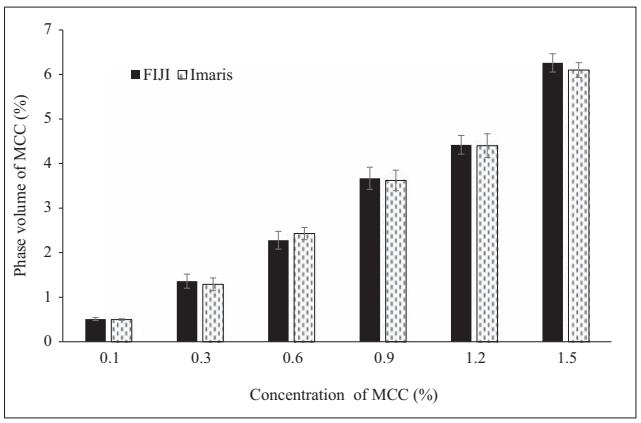

Fig. 7 Phase volume estimates plotted against MCC concentrations in mixture with 1% (w/w) agarose determined by analysing 3D CLSM images using image analysis software – FIJI and Imaris

customisability, which may affect their capacity in estimating phase volume in more complex systems, for example, in tertiary preparations of protein, polysaccharide and a lipid phase.

Conclusions

Rheology-based blending laws have been used extensively in the literature to predict the mechanical strength of synthetic polymer matrices, and this is augmented in biomaterial composite gels by the estimation of solvent partition between polymeric phases, since these are largely aqueous preparations. Nevertheless, such attempts are built around painstaking rheological experimentation and they also require considerable modelling expertise, hence making it difficult for laboratories to implement or reproduce. Given this, the suitability of CLSM based 3D imaging, coupled with image analysis, in quantifying phase volumes in a binary mixture was investigated as a rapid alternative approach. The microscopic protocol could successfully render phase volumes of hydrated MCC particles suspended in an agarose network, an outcome that agreed remarkably well with those obtained from rheological modelling. The protocol could cope with increasing concentrations/density of the filler phase in phase volume estimation and merits further consideration in more complex preparations.

Acknowledgements The authors acknowledge the facilities and technical assistance of the RMIT University's Microscopy and Microanalysis Facility.

References

1. K. Prameela, C.Murali Mohan, C. Ramakrishna, Chap. 1 - *Biopolymers for Food Design: Consumer-Friendly Natural Ingredients*, in *Biopolymers for Food Design*, ed. by A.M. Grumezescu, A.M. Holban (Academic Press, Cambridge, 2018), p. 1–32
2. C. Stenger et al., Formation of concentrated biopolymer particles composed of oppositely charged WPI and pectin for food applications. J. Dispersion Sci. Technol. **38**(9), 1258–1265 (2017)
3. V. Tolstoguzov, Ionic strength and poly ion charges. Int. Food Ingred. **2**, 8–9 (1990)
4. M.M.G. Koning, J. van Eendenburg, D.W. de Bruijne, *Mixed Biopolymers in Food Systems: Determination of Osmotic Pressure*, in *Food Colloids and Polymers*, ed. by E. Dickinson, P. Walstra (Woodhead Publishing. Cambridge, 2005), p. 103–112
5. T. Giancone et al., Protein–polysaccharide interactions: Phase behaviour of pectin–soy flour mixture. Food Hydrocoll. **23**(5), 1263–1269 (2009)
6. P.D. Pudney, T.M. Hancewicz, D.G. Cunningham, The use of confocal Raman spectroscopy to characterise the microstructure of complex biomaterials: foods. J. Spectrosc. **16**(3–4), 217–225 (2002)
7. L.E. Nielsen, in *Morphology and the elastic modulus of block polymers and polyblends*, in *Rheological Theories· Measuring Techniques in Rheology Test Methods in Rheology· Fractures Rheological Properties of Materials· Rheo-Optics· Biorheology*. (Springer, Berlin, 1975), p. 594–600
8. M. Takayanagi, H. Harima, Y. Iwata, Viscoelastic behaviour of polymer blends and its comparison with model experiments. Mem. Fac. Eng. Kyusha Univ. **23**, 1–13 (1963)
9. X. Li et al., Studies of phase separation in soluble rice protein/different polysaccharides mixed systems. LWT Food Sci. Technol. **65**, 676–682 (2016)
10. T. Moschakis et al., in Microrheology and microstructure of water-in-water emulsions containing sodium caseinate and locust bean gum. Food Funct. **9**(5), 2840–2852 (2018)
11. H. Pan et al., Effect of the extent and morphology of phase separation on the thermal behavior of co-blending systems based on soy protein isolate/alginate. Food Hydrocoll. **52**, 393–402 (2016)
12. N. Lorén, M. Langton, A.M. Hermansson, Confocal laser scanning microscopy and image analysis of kinetically trapped phase-separated gelatin/maltodextrin gels. Food Hydrocoll. **13**(2), 185–198 (1999)
13. J.C.G. Blonk et al., A new CSLM-based method for determination of the phase behaviour of aqueous mixtures of biopolymers. Carbohyd. Polym. **28**(4), 287–295 (1995)
14. P. Mhaske et al., Quantitative analysis of the phase volume of agarose-canola oil gels in comparison to blending law predictions using 3D imaging based on confocal laser scanning microscopy. Food Res. Int. **125**, 108529 (2019)
15. J. Nsor-Atindana et al., Functionality and nutritional aspects of microcrystalline cellulose in food. Carbohyd. Polym. **172**, 159–174 (2017)
16. N. Russ et al., Influence of nongelling hydrocolloids on the gelation of agarose. Biomacromolecules **14**(11), 4116–4124 (2013)
17. C. Kyomugasho et al., Evaluation of cation-facilitated pectin-gel properties: Cryo-SEM visualisation and rheological properties. Food Hydrocoll. **61**, 172–182 (2016)
18. X. Qi et al., Facile formation of salecan/agarose hydrogels with tunable structural properties for cell culture. Carbohyd. Polym. **224**, 115208 (2019)
19. V. Zamora-Mora et al., Chitosan/agarose hydrogels: Cooperative properties and microfluidic preparation. Carbohydr. Polym. **111**, 348–355 (2014)
20. C.P. Azubuike, A.O. Okhamafe, Physicochemical, spectroscopic and thermal properties of microcrystalline cellulose derived from corn cobs. Int. J. Recycl. Org. Waste Agric. **1**(1), 9 (2012)
21. H. Toğrul, N. Arslan, Flow properties of sugar beet pulp cellulose and intrinsic viscosity–molecular weight relationship. Carbohyd. Polym. **54**(1), 63–71 (2003)
22. M. Murigi et al., Comparison of physicochemical characteristics of microcrystalline cellulose from four abundant Kenyan biomasses. IOSR J. Polym. Text. Eng. **1**(2), 53–63 (2014)
23. A.J. Gravelle, S. Barbut, A.G. Marangoni, Food-grade filler particles as an alternative method to modify the texture and stability of myofibrillar gels. Sci. Rep. **7**(1), 11544 (2017)
24. C. Semasaka et al., Modeling water partition in composite gels of BSA with gelatin following high pressure treatment. Food Chem. **265**, 32–38 (2018)
25. L.W. Koh, S. Kasapis, Orientation of short microcrystalline cellulose fibers in a gelatin matrix. Food Hydrocoll. **25**(5), 1402–1405 (2011)
26. A.A. Karamitrou, G.N. Tsokas, M. Petrou, A pixel-based semi-stochastic algorithm for the registration of geophysical images. Archaeol. Prospect. **24**(4), 413–424 (2017)
27. T.Y. Goh et al., Performance analysis of image thresholding: Otsu technique. Measurement **114**, 298–307 (2018)